

# Consequent Pole Permanent Magnet Machine with Field Weakening Capability

Juan A. Tapia  
Dept. of Electrical Engineering  
University of Concepcion  
Casilla 160-C, Correo 3  
Concepcion, CHILE

Franco Leonardi  
Vehicle Electronic Systems  
Department  
Ford Research Laboratories  
Dearborn MI  
Ph./fax 313-390 6923

Thomas A. Lipo, *Fellow*, IEEE  
Dept. of Electrical and Computer Engineering  
University of Wisconsin-Madison  
1415 Engineering Dr  
Madison WI 53706-1651 USA  
Tel:(608) 265-0727 Fax(608) 262-5559

**Abstract:** The electromagnetic design procedure and laboratory test results are presented in this paper for a Consequent Pole Permanent Machine (CPPM) with Field Weakening Capability. Due to its particular configuration, the CPPM allows one to easily control the air-gap flux in a wide range so that the speed range of the machine is increased. Two components of the flux: one -almost constant- coming from the permanent magnet located in the rotor surface of the machine and the other -variable- coming from a field winding located in the middle of the stator, converge in the air-gap, characterizing the level of excitation of the machine. Preliminary 3D finite element analysis results establish that with 10% of the phase MMF, it is possible to vary the flux in a wide range. A 3KW, 1000 to 3000 RPM velocity range, 8 pole and 32 AC volt generator using this configuration is tested to verify the flux control capability of this structure.

## I. INTRODUCTION

In the last decades PM machine drives have increased their popularity in a wide variety of industrial applications for a number of reasons, e.g. higher power density and efficiency, higher reliability and, lower inertia. However, fixed excitation provided for the PM limits the power capability of the drive. In fact, the necessary power electronic converter to transform the fixed utility frequency into variable frequency and voltage to supply the machine [1] imposes voltage and current restrictions [2]. Therefore, to extend the speed range PMAC drives are operated with volt per hertz constant ratio up to base speed and with constant voltage and field weakening at higher speed.

To reduce the excitation at high speed, vector control techniques impose a demagnetizing field along to the *d*-axis [3,4,5] using stator current control. In that manner, interior and surface PM machine can work over the rated speed. However, this mechanism involves a risk to irreversible demagnetization of the permanent magnet pieces and generation of heat due to the  $I^2R$  losses. If the temperature and reverse *d*-axis flux are high enough to move the operating point near or below of the knee of the normal demagnetization irreversible changes in the PM properties take effect.

To avoid this undesirable effect, alternative solutions have been reported. [6] suggests connecting groups of the stator

winding in different configurations so that the induced voltage is adjusted accordingly. In [7] a stator mounted PM machine is presented where the weakening process is obtained changing the reluctance path of the magnet. Using a field winding to add or subtract flux from the PM is explained in [8]. In this case, magnet and winding control are located in the stator [9]. A Synchronous PM motor with two-section rotor with field weakening is analyzed. Here, the reluctance of the *d*-axis flux path is varied, changing the ratio between each section.

The purpose of this paper is to explore a magnetic structure called Consequent Pole Permanent Magnet (CPPM) Machine with field weakening capability, Fig. 1. This combines the fixed excitation of the earth rare permanent magnet with the variable flux given by a field winding. In that way, airgap flux can be controlled in a wide range with minimum of conduction losses and without demagnetizations risk for the PM pieces. Finite element analysis establishes for a 3KW prototype using this configuration, that less than 10% of the AC winding mmf is necessary to vary the airgap flux in a +/- 50% range. An optimized AC generator using sizing equation analysis, has been built based on this concept. In the following section, a description and operating principles are explained and optimization process is shown.

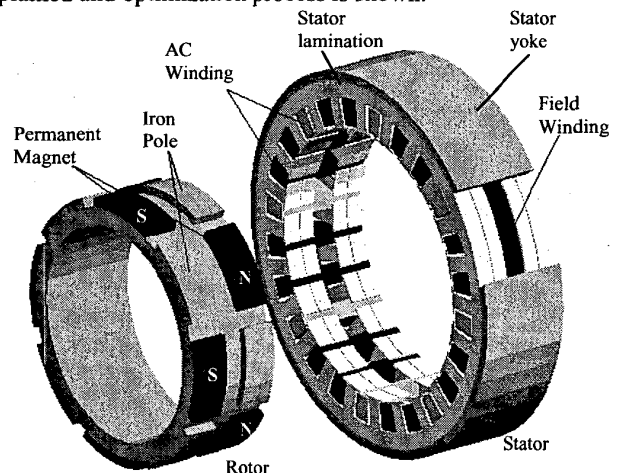


Fig. 1. 8-poles CPPM machine structure.

## II. DESCRIPTION

Fig. 1 shows the structure of the CPPM machine. The machine consists of a two-rotor section with partial surface-mounted permanent magnets structure, which are radially and consequently magnetized. One stator with partial solid yoke to diminish the interlamination airgap and a conventional three-phase winding. Additionally, a circumferential field winding in the middle of stator provides a variable excitation.

The radial magnetization of the permanent magnets creates an almost constant flux, which circulates from one pole to the next one across the stator and rotor yoke, teeth a PM pieces. This portion of the flux is determined mainly for the PM's geometry and the reluctance of its path. In this case, the air-gap and magnet reluctances are the most important values. On the other hand, injecting DC current in to field winding, generates a flux which goes from the one iron pole to another through the stator and rotor yoke, with a path entirely composed of this material, except the main air-gaps. Due to the comparative low reluctance of this path, the DC current flowing for the field winding can easily control this flux. The combination of these two fluxes produces a variable level of excitation in the machine according with the magnitude and direction of the DC current. Fig 2, outlines the per pole flux path under different DC field current.

- For no field current, the flux in the machine is only due to the PM and, because the magnetization is consecutive, the trajectory of the flux from one section to the next one crosses the stator yoke the in oblique direction. Fig. 2a.

- When the flux generated by the field winding flows in the direction where is added to the PM's, the flux closes its path in the same magnetic pole, Fig.2b. That means, that in the airgap, flux coming from the PM and the fields are in opposite directions. As a result, the total flux per pole decreases as the field flux increases. Flux crosses the stator yoke axially.

- If the field current is reversed the field flux changes its direction and at the total airgap flux is the summation of both components. Therefore, as the field current increases, the flux per pole increases. Flux closes its path crossing the stator yoke azimuthally. Fig. 2c.

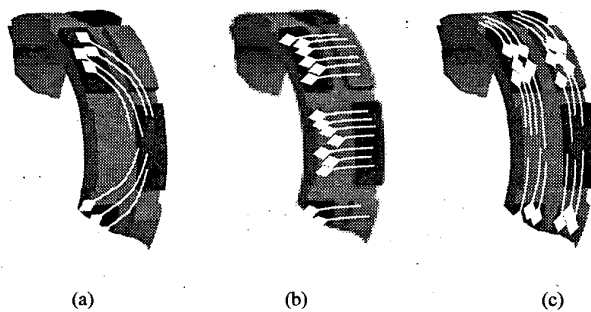


Fig. 2. Flux distribution in the CPPM

The Consequent Pole Permanent Magnet machine presents several advantages in comparison with the regular PM machine such as:

- Wide range of airgap flux control to reduce or increase its value. This is accomplished with a low requirement for field ampere-turns.
- This particular configuration permits one to control the level of excitation of the machine without any demagnetization risk for the permanent magnet parts.
- Airgap flux control allows one to increase and to improve the power capability at low, medium and high-speed range of the drive-motor configuration

## III. SIZING EQUATION ANALYSIS

In order to obtain adequate dimensions for the prototype to build a set of equation are derived to relate mechanical dimensions, electromagnetic restrictions and technical constraints. Finally an optimization based on surface current density is carried out to obtain optimum  $D_i/D_o$  ratio.

Dividing the airgap surface in two sections, one corresponding to the permanent magnet and the other one to the iron pole areas, the total airgap flux can be divided in two components associated to each of these sections. If excitation current of the field winding is injected, with a positive or negative polarity, flux of the iron pole section will change linearly if the reluctance of the iron is neglected. On the other hand, flux associated with the permanent magnet will be invariant. Superposition of these two fluxes results in the total airgap flux. This resultant flux can be the either the summation or subtraction of the each component.

Analyzing the actual flux distribution in the previous section, it is found that due to the necessary space required to allocate the field winding, the most restricted path for the yoke flux is when fluxes are subtracting flowing from the permanent magnet to the iron pole, Fig. 3. In effect, according with Fig. 4, the total area to circulate the flux for this operating condition is reduced to that defined by  $d_c$ .

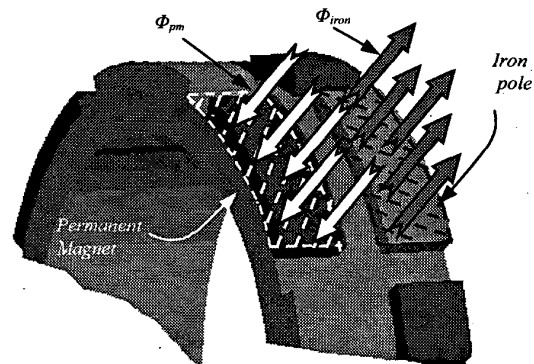


Fig. 3. Flux distribution in the airgap for case b) fig. 2

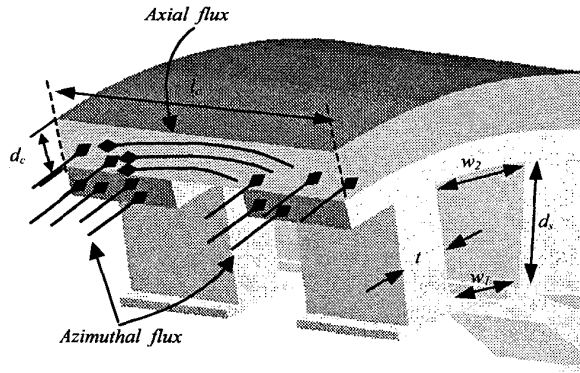


Fig. 4. Flux path in the stator yoke

Following the procedure given by Honsinger and Lipo in [10] and [11] sizing equations are obtained considering this extreme operating condition. Based on maximum values of flux density in the airgap  $B_{gap}$ , stator tooth  $B_{tooth}$ , and yoke  $B_{yoke}$ , expression for teeth width and axial stator yoke thickness are given for equations (1) and (2)

$$t = \frac{B_{gap}}{B_{tooth}} \frac{D_i}{K_s S_1} \pi \quad (1)$$

$$d_c = \frac{B_{gap}}{B_{yoke}} \frac{D_i}{2} K_a \quad (2)$$

$D_o$  : Outer diameter

$D_i$  : Airgap diameter

$K_s$  : stack factor which take into account inter-lamination airgap.

$p$  : number of pole of the machine

$S_1$  : number of stator slot

and  $K_a$  is defined in term of  $l_e$  : stack length of the machine

$$K_a = \frac{l_e}{D_o} \quad (3)$$

This index is referred as 'external aspect ratio' and represents the proportion between the axial length (active length) and the outer diameter of the machine. For a regular radial machine, it is usual to define the 'aspect ratio', which is the proportion between axial length and airgap diameter. For the CPM the analogous index is directly related with the external dimension of the machine.

Notice that  $d_c$  does not depend of the number of poles as for a radial machine. In fact, as the number of pole increase in a regular radial or axial flux machine, the amount of flux per pole is reduced if the peak flux density is the same [12], therefore the yoke thickness can be smaller reducing the outer diameter. However, in the CPM for a fixed outer diameter, as  $K_a$  increases the amount of flux per pole also increases (larger value of  $l_e$ ), as a result stator yoke increases its thickness and

the inner diameter has to decrease to maintain a reasonable value of  $B_{yoke}$ .

The slot geometry, according Fig. 4 is given by:

$$w_1 = D_i \frac{\pi}{S_1} - t \quad (4)$$

$$w_2 = (D_o + 2d_c) \frac{\pi}{S_1} - t \quad (5)$$

Using the fact, that

$$D_o = D_i + 2(d_s + d_c) \quad (6)$$

the tooth length can be expressed, using (4) and (5) as

$$d_s = (w_2 - w_1) \frac{S_1}{2\pi} \quad (7)$$

Finally, for a trapezoidal geometry of the stator slot (fig. 4), the slot area can be expressed in terms of the equations (4), (5) and (7) like

$$A_{slot} = (w_1 + w_2) \frac{d_s}{2} = \frac{\pi}{4S_1} (a D_i^2 - 2b D_i D_o + D_o^2) \quad (8)$$

Where

$$a : 2G_t + 2G_c G_t K_a + G_c^2 K_a^2 \quad (9)$$

$$b : G_t + G_c K_a \quad (10)$$

$G_t$  and  $G_c$  are defined as the flux density ratio of the tooth and stator yoke:

$$G_t = \frac{B_{gap}}{B_{tooth} K_s} \quad (11)$$

$$G_c = \frac{B_{gap}}{B_{yoke}} \quad (12)$$

Dividing both side of (8) by  $D_o^2$ , this expression can be written like

$$\frac{A_{slot} S_1}{\left(\frac{D_o^2 \pi}{4}\right)} = a \left(\frac{D_i}{D_o}\right)^2 - 2b \left(\frac{D_i}{D_o}\right) + 1 \quad (13)$$

Equation (13) has similar structure to the expression found in [10]. The right side corresponds to the ratio between the total stator surface to locate the copper of the AC winding and the total transversal area of the machine. The left side is a quadratic equation, which is function of the ratio  $D_i/D_o$ . Setting adequate flux density values for each portion of the magnetic circuit of the machine and selecting  $K_a$  based on a desired external aspect ratio, the function defined by (13) can be optimized so that maximize the airgap.

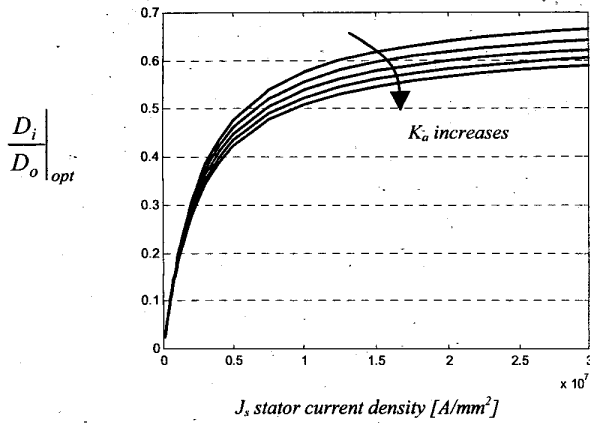


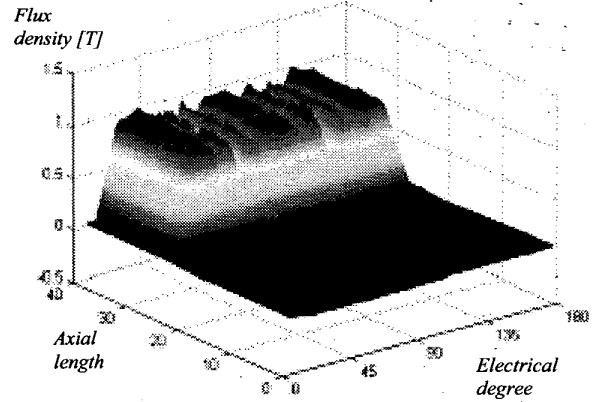
Fig. 5. Optimum Di/Do ratio.  $\frac{B_{gap}}{B_{tooth}} = 0.4$ ,  $\frac{B_{gap}}{B_{core}} = 0.5$ ,  $D_o = 168\text{mm}$

Fig. 5 is the output of the optimization algorithm. As expected, increasing the external aspect ratio,  $K_a$ , the stator yoke thickness also increases, as a result the optimum diameter ratio  $D_i/D_o$  decreases. CPM with larger stack length reduces the inner diameter.

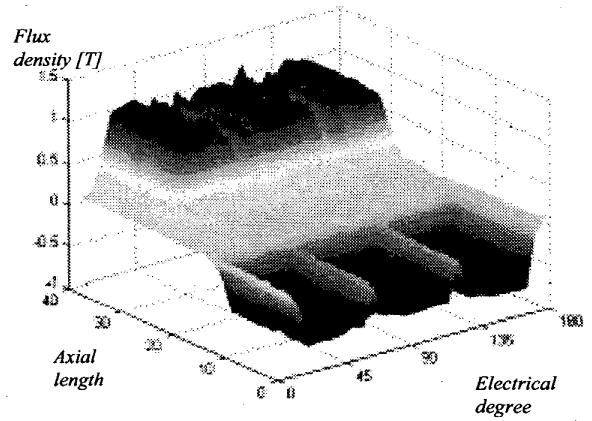
#### IV. FINITE ELEMENT ANALYSIS

To find out the flux distribution and the field weakening capability of the prototype a 3D finite element (FE) analysis was carried out. The main goal of this investigation is to determine the size of the field winding, which can not be estimated with the sizing equations developed. In effect, non-linearity of the iron is not considered in the previous section and defines the size of the stator yoke and the necessary ampere-turns of the excitation winding to control the airgap flux.

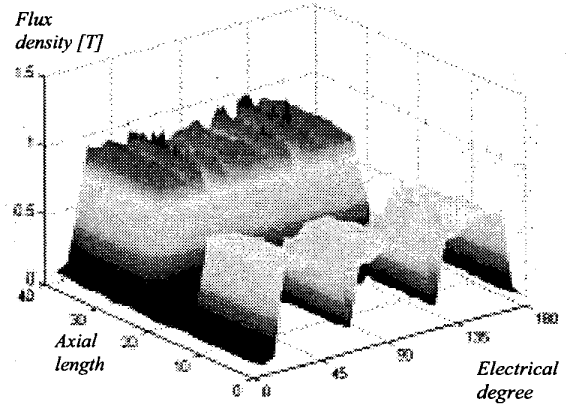
Fig. 6 airgap flux is shown for three different conditions of the field current. From this, it is possible to see that the flux over the PM is uni-directional and its magnitude is almost constant, however the direction of the flux over the iron pole surface changes according with the direction field excitation. These two components make the total airgap flux vary weakening or boosting the field from the non-current condition. Analyzing both fluxes separately, Fig. 7, it can be noticed that the PM does not maintain a constant value of flux due to the saturation of the iron. With a variation of +/- 500 AT the flux can be modified in a range from 1.7 to 8.1 mWb (Fig. 7). With an adequate value of the current density an estimation of the size required to allocate the excitation winding can be calculated.



(a)



(b)



(c)

Fig. 6. Airgap flux distribution for different field AT. a) No field current, b) -500 AT, c) 500 AT

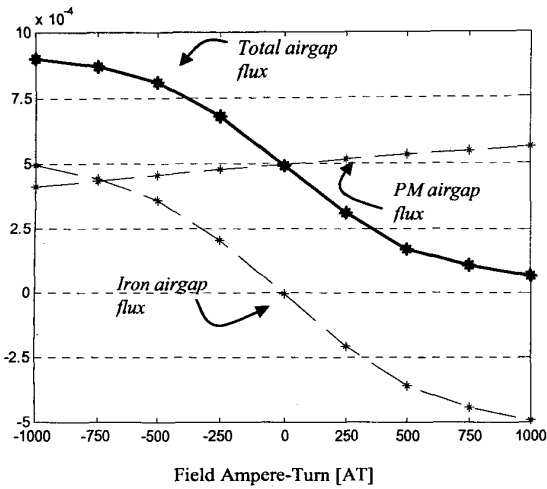


Fig. 7. Flux distribution in the airgap

Fig. 8 shows the variation of the flux, crossing the stator yoke in axial direction. When fluxes of each portion of the airgap are in the opposite direction, this core flux became bigger. Appropriate value of the flux density defines the area of the axial yoke. This dimension plus the volume to locate the winding redefines the stator geometry.

Based on the previous sizing equation optimization process and the 3D FE analysis to calculate the mmf field required a 3KW 8-poles machine is designed using the consequent poles structure. Main data of the prototype are shown in Table I. Fig. 9 shows the CPM prototype that was tested.

TABLE I: PROTOTYPE DATA		
Stator Outer Diameter	168	mm
Stator Inner Diameter	118.2	mm
Stack length	40	mm
Slot depth	13.7	mm
Tooth width	6.9	mm
Axial length of the PM ( $l_{ep}$ )	15	mm
Width of the PM	5	mm
Poles number	8	
Number of phases	3	

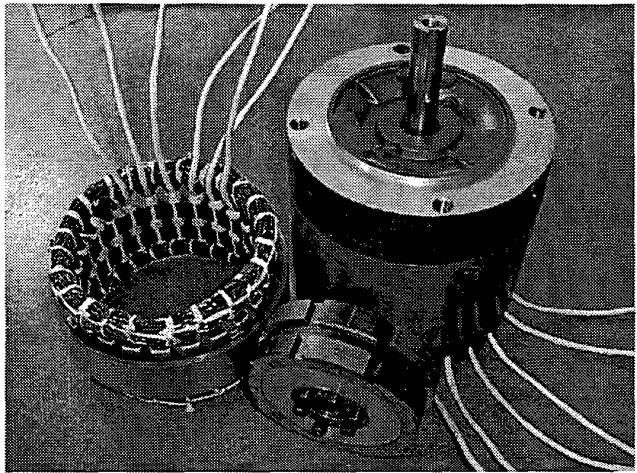


Fig. 9. Consequent Pole Permanent Magnet Machine 3KW prototype

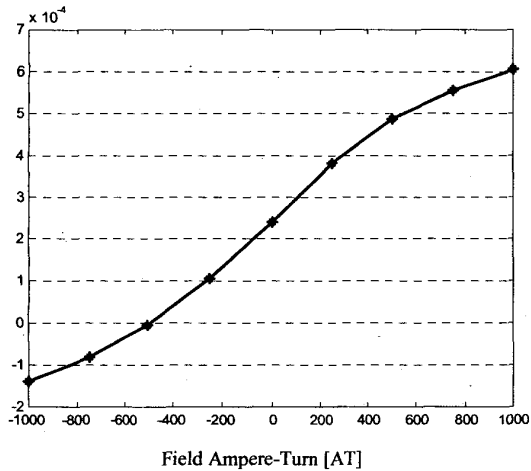


Fig. 8. Flux crossing stator yoke in axial direction

## V. EXPERIMENTAL RESULTS

Fig 10 shows the field control capability of the CPPM machine. While is spinning at 1500 rpm three open circuit phase voltages for different conditions of the field current were obtained. With a variation of the  $\pm 300$  AT the flux is modulated over a range  $\pm 25\%$  respect to no field current. This result is lower that FE analysis predicts. In fact, over  $\pm 40\%$  of the airgap flux variation for the same field AT range is expected in the theoretical approach.

A comparison between the experimental prototype and FE analysis model for the flux per pole is shown in Fig. 11. It is clear that the slope of the actual flux-field mmf is smaller than the computational model, which means that extra airgaps are not considered, such as stator and rotor lamination-yoke junctions. However, when field mmf is zero, both curves are coincident, and the permanent magnet flux estimation result correct.

21-Mar-81  
17:34:08

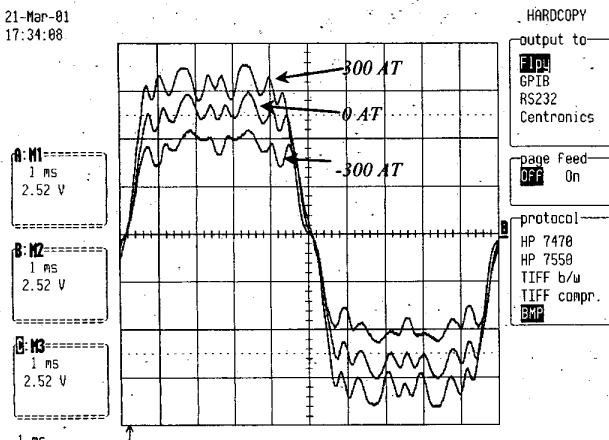


Fig. 10. AC Phase voltage output of the CPM for different field ampere-turns (no-load condition)

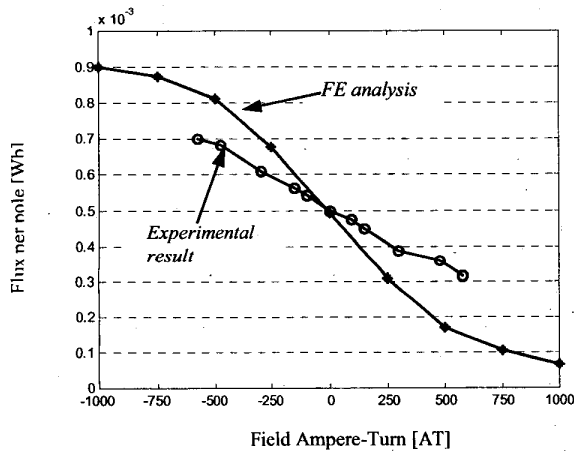


Fig. 11. Experimental result comparison for the airgap flux

## VI. CONCLUSIONS

This paper describes the operating principles; optimization process; finite element analysis and the prototype performance of the Consequent Pole Permanent Magnet machine. This machine configuration controls the flux in the airgap without affecting the magnetization characteristics of the permanent magnets pieces. The flux in the airgap is

determined by the direction and magnitude of the field DC current, which circulates in a stationary winding located in the middle of the stator.

Design procedure using new set of sizing equation technique, 3D finite element analysis are used to obtain optimum values for the geometry of this field winding, the stator yoke bridge in order to maximize the efficiency and power density for a particular application.

Experimental results establish moderate correlation with finite element analysis. Airgap between stator lamination and yoke introduce an extra reluctance that has to be considered. And the disagreement between both curves are related with the variable excitation provide for the field winding

## VII. REFERENCES

- [1] T.M. Jahns, "Motion Control with Permanent-Magnet AC Machines," *Proceeding of the IEEE* Vol 82, NO.8, August 1994. pp 1241-1252.
- [2] L. Xu, et al, "A New Design Concept of Permanent Magnet Machine for Flux Weakening Operation," *IEEE Transaction on Industry Application*, Vol. 31 No. 2 March/April 1995 pp.373-378
- [3] Y. Sozer, D.A. Torrey, "Adaptive Flux Weakening Control of Permanent Magnet synchronous Motor" *IEEE Industrial Application Society Conference Meeting*, St Louis 1998.
- [4] W. L. Soong, T.J Miller, 'Field-Weakening Performance of brushless Synchronous AC Motor Drives' *IEE Proceeding Electric Power Application*, Vol. 141, No. 6, November 1994, pp 331-340
- [5] S. R. Macminn, T. M. Jahns, "Control Techniques for Improved High-Speed Performance of Interior PM Synchronous Motor Drives" *IEEE Transactions on Industry Applications*. VOL 27, NO. 5, September/October 1991
- [6] E. Nipp, "Alternative to Field-Weakening of Surface-Mounted Permanent-Magnet Motors for Variables-Speed Drives." *Conference record of the IAS '95 Annual Meeting*, 1995.
- [7] A. Shakal, Y. Liao, T. A. Lipo, "A Permanent Magnet AC Machine Structure with True Field Weakening Capability." *Conference record of the IEEE International Symposium Industrial Electronics*, 1993
- [8] F. Leonardi, P. J. McCleer, T. Lipo, "The DSPM: An AC Permanent Magnet Traction Motor with True Filed Weakening" *2nd International Conference on "All Electric Combat Vehicle"*, Detroit MI, June 1997.
- [9] B.J. Chalmers, R. Akmese, L. Musaba, "Design and Field-Weakening Performance of Permanent-Magnet/Reluctance Motor with Two-Part Rotor." *IEE Proceeding Electric Power Application*. Vol. 145, No. 2, march 1998.
- [10] V.B. Honsinger, "Sizing Equations for Electrical Machinery," *IEEE Transactions on Energy Conversion*. Vol. EC-2, No. 1, March 1987. pp 116-121
- [11] T.A. Lipo. "Electromechanical Machine Design," *Classroom text for ECE 713*, University of Wisconsin-Madison 1995.
- [12] F. Liang, D.W. Novotny, R. Fei, X. Xu, "Selection of the Pole Number of Induction Machines for Variable Speed Applications," *IEEE Transactions on Industry Applications*. Vol 31, No. 2, March/April 1995 pp 304-310.